Amyloids

International Edition: DOI: 10.1002/anie.201511099
German Edition: DOI: 10.1002/ange.201511099

# Enhanced Fibril Fragmentation of N-Terminally Truncated and Pyroglutamyl-Modified Aβ Peptides

*Melanie Wulff, Monika Baumann, Anka Thümmler, Jay K. Yadav, Liesa Heinrich, Uwe Knüpfer, Dagmar Schlenzig, Angelika Schierhorn, Jens-Ulrich Rahfeld, Uwe Horn, Jochen Balbach, Hans-Ulrich Demuth, and Marcus Fändrich**

***Abstract:*** *N-terminal truncation and pyroglutamyl (pE) formation are naturally occurring chemical modifications of the Aβ peptide in Alzheimer's disease. We show herein that these two modifications significantly reduce the fibril length and the transition midpoint of thermal unfolding of the fibrils, but they do not substantially perturb the fibrillary peptide conformation. This observation implies that the N terminus of the unmodified peptide protects Aβ fibrils against mechanical stress and fragmentation and explains the high propensity of pE-modified peptides to form small and particularly toxic aggregates.*

**N**-terminal truncation and pE modification of the Aβ peptide define the biochemical staging and progression of Alzheimer's disease (AD).[1–3] Depending on the type of analysis, 10–50 % of the deposited Aβ is pE-modified in human AD.[4–6] Pharmacological inhibition of glutamyl cyclase, the enzyme that catalyzes the formation of the pE lactam ring, reduces amyloid plaque deposition in vivo and retards memory decline in mice,[1] but mixed results have been published on the biophysical effects of these modifications. Several studies report pyroglutamylated Aβ to exhibit accelerated fibril formation;[7–10] while others claim inhibitory activities,[11] an enhanced propensity to form small, cytotoxic oligomers,[8,10,12,13] or differential effects on the Aβ40 and Aβ42 peptide variants.[14]

To clarify the kinetic effect of N-terminal modification on Aβ fibrillogenesis, we used real-time thioflavin T (ThT) fluorescence measurements. We found that N-terminal truncation accelerates fibril formation and this effect is even more enhanced in the presence of a pE lactam ring (Figure 1). We used disaggregated peptides in our measurements and performed five or more replicates per condition to account for the known scatter of ThT kinetics data.[15] The enhancement effect was observed independent of whether the analyzed series of peptides extended up to residue 40 or 42 (Figure 1 B). Modification uniformly reduced the lag time $t_{lag}$ while increasing the growth rate constant $k$ (Figure S1 in the Supporting Information). These data show that the two chemical modifications accelerate the lag phase as well as the growth phase of fibril formation.

We obtained no evidence that our results are influenced by aberrant pE ring-forming or ring-opening reactions during peptide disaggregation or fibril formation reactions, since mass spectrometry showed identical peptide masses before and after these treatments (Figure S2). Critical-concentration measurements, in which we determined the Gibbs free energy ($\Delta G$) of Aβ(1–40), Aβ(3–40), and pEAβ(3–40) aggregation to be $-34.7 \pm 0.2$ kJ mol$^{-1}$, $-36.3 \pm 0.1$ kJ mol$^{-1}$, and $-35.9 \pm 0.3$ kJ mol$^{-1}$, respectively, revealed that N-terminal modifications make aggregation thermodynamically slightly more favorable. Hence, N-terminal modification affects both the kinetics and the thermodynamics of fibril formation.

Analysis of the secondary structure of the disaggregated peptides with far-ultraviolet circular dichroism (CD) spectroscopy revealed similar spectral characteristics for the Aβ(1–40), Aβ(3–40), and pEAβ(3–40) peptides (Figure S3). We found strong ellipticity minima at 200 nm that, taken together with previous nuclear magnetic resonance (NMR) measurements,[16] indicate the presence of a monomeric peptide with random-coil-like conformation. Analysis of the fibril state with attenuated total reflectance Fourier-transform

[*] M. Wulff, Prof. Dr. M. Fändrich
Institute for Pharmaceutical Biotechnologie, Ulm University
Helmholtzstrasse 8/1, 89081 Ulm (Germany)
E-mail: marcus.faendrich@uni-ulm.de
A. Thümmler
Probiodrug AG, Biocenter
Weinbergweg 22, 06120 Halle (Saale) (Germany)
M. Baumann, Prof. Dr. J. Balbach
Institute of Physics, Martin Luther University Halle-Wittenberg
Betty-Heimann-Strasse 7, 06120 Halle (Saale) (Germany)
Dr. J. K. Yadav
Department of Biotechnology, School of Life Sciences
Central University of Rajasthan
NH-8, Ajmer-305801, Rajasthan (India)
L. Heinrich, U. Knüpfer, Dr. U. Horn
Leibniz Institute for Natural Product Research and Infection Biology
Hans Knöll Institute, Beutenbergstrasse 11a, 07745 Jena (Germany)
D. Schlenzig, Dr. J.-U. Rahfeld, Prof. Dr. H.-U. Demuth
Department of Drug Design and Target Validation MWT Halle/Saale
Fraunhofer Institute for Cell Therapy and Immunology IZI Leipzig
Biocenter, Weinbergweg 22, 06120 Halle (Saale) (Germany)
Dr. A. Schierhorn
Service Unit for Mass Spectrometry
Martin Luther University Halle-Wittenberg
Kurt-Mothes-Strasse 3, 06120 Halle (Saale) (Germany)
A. Thümmler
Current address: Nomad Bioscience GmbH, Biocenter
Weinbergweg 22, 06120 Halle (Saale) (Germany)

Supporting information for this article can be found under: http://dx.doi.org/10.1002/anie.201511099.

  

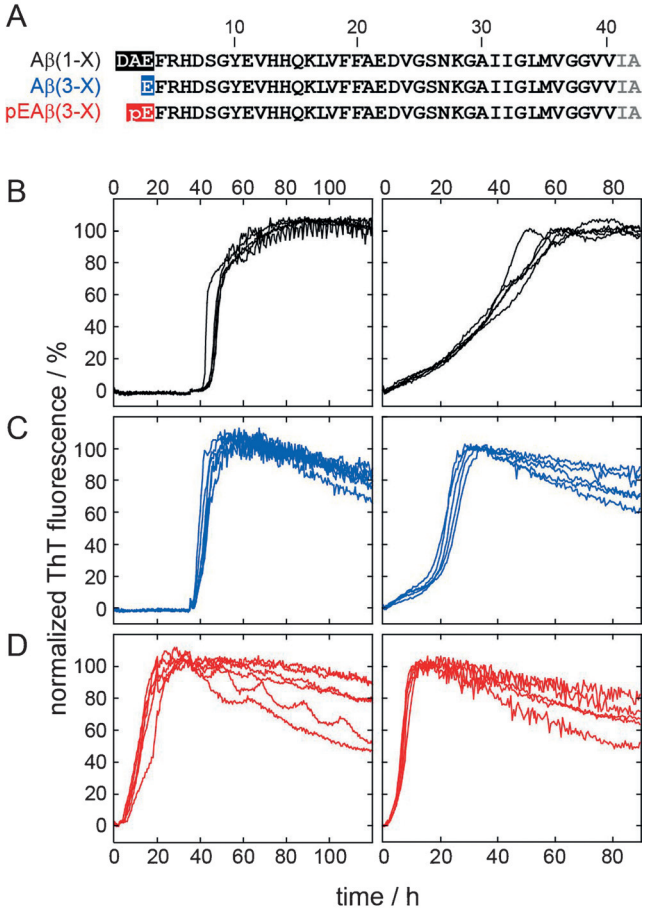


***Figure 1.*** N-terminal modification accelerates Aβ fibrillation. A) Amino acid sequences of the Aβ peptides investigated in this study. B–D) ThT-based aggregation kinetics measurements of Aβ(1–*X*) (B), Aβ(3–*X*) (C), and pEAβ(3–*X*) (D) show the effect of N-terminal modification. Left column: Aβ peptides extending up to residue 40. Right column: Aβ peptides extending up to residue 42 ($n = 5$–6). Aggregation kinetics were perfomed at 37 °C in 50 mM sodium phosphate buffer (pH 7.4) and 20 μM Aβ peptide. Color coding: Aβ(1–*X*) black, Aβ(3–*X*) blue, and pEAβ(3–*X*) red.

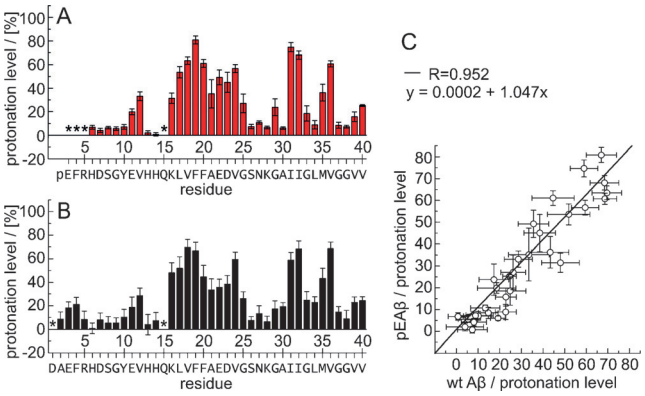


***Figure 2.*** Quantified residue-specific protonation levels after HX for pEAβ(3–40) (A) and Aβ(1–40) (B). Asterisks mark residues that could not be analyzed owing to lack of cross-peak assignments. C) Correlation plot of the protonation data. Linear regression and R value were derived by a least squares linear fit. Error bars show the standard deviation ($n = 3$).

infrared spectroscopy (FTIR) showed the amide I spectral regions to be associated with maxima at around 1630 $cm^{-1}$ (Figure S4A, Table S1). X-ray diffraction (XRD) measurements carried out with fully hydrated fibrils uniformly showed reflections at approximately 4.7 and 10 Å (Figure S4B, Table S1). Moreover, all fibrils showed similar binding to fibril-specific reagents, such as Congo red (Figure S4C,D), ThT dyes (Figure S4E), and the antibody reagent B10AP (Figure S4F).

We then established a recombinant expression system for pEAβ(3–40) and obtained uniformly $^{15}N$-labelled pyroglutamylated Aβ. The recombinant expression system is a prerequisite for performing hydrogen-exchange NMR measurements (Figure S5A,B) to identify the fibril cross-β conformation based on retarded exchange of the backbone amide protons with deuterium.[17–19] We found that pEAβ(3–40) fibrils show a high degree of protection from exchange at discrete sites, specifically involving residues 17–25 and positions 31, 32, 35, and 36 (Figure 2A). For residue 3–5, no residue-specific information was obtained owing to a lack of cross-peak assignments. The exchange-protected regions are very similar to those observed in reference measurements with Aβ(1–40) (Figure 2B,C). While these NMR, XRD, FTIR, and ligand-binding data show that modified and unmodified fibrils comprise similar peptide conformations, transmission electron microscopy (TEM) reveals substantial differences in the overall structures of the formed fibrils. Aβ(3–*X*) and pEAβ(3–*X*) fibrils were significantly shorter than Aβ(1–*X*) filaments, and we observed this effect with different batches of peptide and series of peptides extending up to $X = 40$ or 42 (Figure 3A–F, Figure S6).

The addition of 5% preformed pEAβ(3–40) or Aβ(1–40) fibrils to solutions of the disaggregated pEAβ(3–40) or Aβ(1–40) peptides did not propagate the fibril length properties to the daughter filaments and showed only small effects on the length distribution (Figure S7). Samples of disaggregated Aβ(1–40) always formed long filaments, whereas disaggregated pEAβ(3–40) uniformly produced short fibrils. We conclude that the fibril length properties do not involve the presence of specific conformations that can be stably propagated to the daughter filament by seeding and rather depend on the incorporation of chemically modified peptide. This conclusion is further substantiated by experiments in which we mixed the two peptides in their disaggregated states and determined the length of the resulting filaments (Figure S8). While pure Aβ(1–40) fibrils show a mean length of more than 2500 nm, this value decreased to approximately 900 nm in the presence of 10% pEAβ(1–40), less than 500 nm with 50% pEAβ, and below 200 nm with 100% pEAβ(3–40). Immunogold labelling and EM confirmed the formation of mixed fibrils and showed binding of Aβ(1–40)- and pEAβ(3–40)-specific antibodies to the same fibrous particle (Figure S9).

Fibrils from pEAβ(3–40) are prone to fragmentation during TEM sample workup, since we frequently saw the disintegration of initially much longer filaments on the EM sample grid (Figure 3G). No comparable EM images were obtained with fibrils from unmodified Aβ, and there was also

  

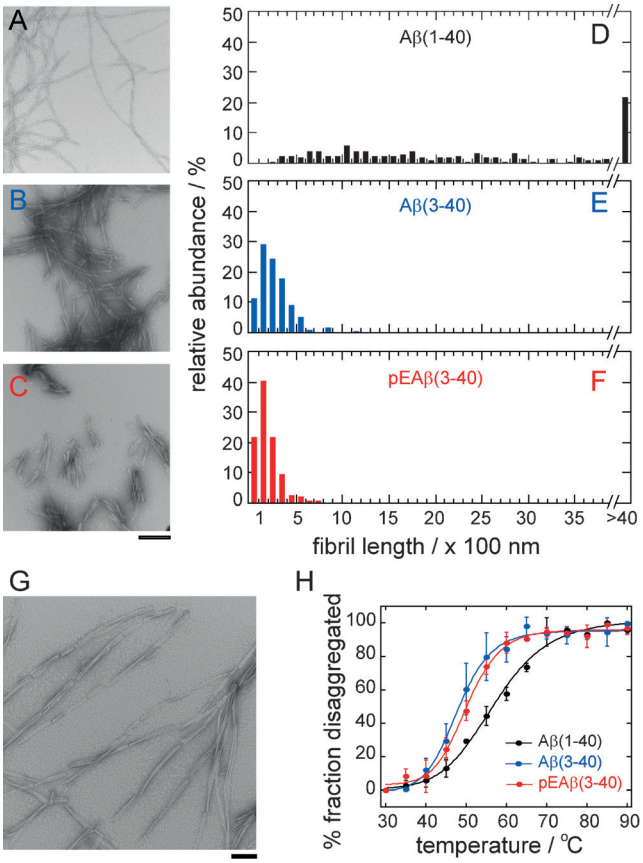


***Figure 3.*** Morphology and structural stability of chemically modified fibrils. A–C) TEM images of Aβ(1–40) (A), Aβ(3–40) (B), and pEAβ(3–40) (C) aggregates. Scale bar: 200 nm. D–F) Histograms of fibril length quantifications from the above TEM images (bin size 100 nm, $n = 200$). G) EM image of pEAβ(3–40) aggregates. Scale bar: 100 nm. H) Thermal stability of the Aβ fibrils, showing the gradual disaggregation (loss of mean residue ellipticity at 220 nm) of the fibrils with increased temperature ($n = 3$).

a strong dependence of the fibril length properties on the agitation strength. The addition of Teflon spheres and increasing the agitation velocity potently reduced the fibril-length distribution (Figure S10), and gradual heating of the fibrils led to a sigmoidal loss of the far-UV CD β-sheet signal at 217 nm (Figure 3H). The temperature midpoint values were 56.6 ± 0.8 °C for Aβ(1–40), 48.7 ± 0.5 °C for Aβ(3–40), and 51.0 ± 0.4 °C for pEAβ(3–40) fibrils. ,Taken together, these data show that modified fibrils show lower resistance to heat denaturation and physical stress than unmodified fibrils.

Our data have several implications. First, they establish that pE modification consistently accelerates Aβ fibrillation in series of peptides extending to positions 40 and 42. We cannot confirm earlier conjectures of differential effects of pyroglutamylation on Aβ(*X*–40) and Aβ(*X*–42) peptides[14] or a possible inhibitory activity of these modifications.[11] Inhibitory activity was previously assumed based on TEM data showing the formation of long filaments to be prevented by pEAβ.[11] While this finding is consistent with the present TEM data that the modified peptides form short fibrils (Figure 3A–C, Figure S6), our thermodynamic measurements establish that the molecular basis of this effect is not prevention of aggregation/fibril formation but increased fragmentation of the formed filaments and a greater susceptibility to mechanical or thermal stress.

Fibril fragmentation was previously identified as a crucial factor in determining the kinetics of fibril formation[20] and the toxicity of the formed aggregates. Small aggregates have a higher specific activity than large aggregates,[21] and numerous publications have shown that the pathogenically most relevant structures of pEAβ are particularly small.[8,12,13] The present demonstration of enhanced fragmentation of aggregates formed from modified Aβ peptides provides a molecular rationale for the ability of this peptide to form cytotoxic structures. However, the lower stability of modified fibrils is less dependent on the presence of a lactam ring than on the simple removal of the two N-terminal residues, since both Aβ(3–*X*) and pEAβ(3–*X*) form short fibrils (Figure 3, Figure S6, $X = 40$ or 42). This finding further suggests that the two N-terminal residues must play a role in stabilizing the fibrils (Figure 3H). Indeed, NMR or cryo-EM studies previously indicated the presence of N-terminal stability in certain Aβ aggregates,[22–24] and solid-state NMR measurements showed higher-order parameters for the first two residues of Aβ(1-40) fibrils than for residue three.[25,26] The peptide thus does not possess a frayed and structurally flexible N terminus and instead participates in the formation of some kind of stable conformation. Moreover, the far N terminus (position 2) represents one of the mutagenic hot spots of the Aβ peptide, with two naturally occurring variants having been described and biophysically characterized.[27] That chemical modifications are able to restrict the fibril length properties is not only relevant for understanding the effects of this naturally occurring modification in the etiology of AD; it also stands as a proof of principle that the length of amyloid structures can readily be manipulated by chemical means. This observation could be also important for the tailored design of peptide assemblies with amyloid-like structures in emerging biotechnological applications.

## Acknowledgements

This work was funded by the German Ministry for Science and Education (ProNet-T3). M.F. has been additionally supported by Deutsche Forschungsgemeinschaft (SFB 610 N01; FA456/12-1).

**Keywords:** amyloids · covalent protein modifications · Alzheimer's disease · peptide aggregation · protein folding

**How to cite:** *Angew. Chem. Int. Ed.* **2016**, *55*, 5081–5084
*Angew. Chem.* **2016**, *128*, 5165–5168

[1] S. Schilling, U. Zeitschel, T. Hoffmann, U. Heiser, M. Francke, A. Kehlen, M. Holzer, B. Hutter-Paier, M. Prokesch, M. Windisch et al., *Nat. Med.* **2008**, *14*, 1106–1111.
[2] A. Rijal Upadhaya, I. Kosterin, S. Kumar, C. A. F. von Arnim, H. Yamaguchi, M. Fändrich, J. Walter, D. R. Thal, *Brain* **2014**, *137*, 887–903.
[3] D. R. Thal, J. Walter, T. C. Saido, M. Fändrich, *Acta Neuropathol.* **2015**, *129*, 167–182.

  

[4] N. Sergeant, S. Bombois, A. Ghestem, H. Drobecq, V. Kostanjevicki, C. Missiaen, A. Wattez, J.-P. David, E. Vanmechelen, C. Sergheraert, A. Delacourte, *J. Neurochem.* **2003**, *85*, 1581 – 1591.
[5] Y.-M. Kuo, M. R. Emmerling, A. S. Woods, R. J. Cotter, A. E. Roher, *Biochem. Biophys. Res. Commun.* **1997**, *237*, 188 – 191.
[6] Y. Harigaya, T. C. Saido, C. B. Eckman, C.-M. Prada, M. Shoji, S. G. Younkin, *Biochem. Biophys. Res. Commun.* **2000**, *276*, 422 – 427.
[7] D. Schlenzig, S. Manhart, Y. Cinar, M. Kleinschmidt, G. Hause, D. Willbold, S. A. Funke, S. Schilling, H.-U. Demuth, *Biochemistry* **2009**, *48*, 7072 – 7078.
[8] D. Schlenzig, R. Rönicke, H. Cynis, H.-H. Ludwig, E. Scheel, K. Reymann, T. Saido, G. Hause, S. Schilling, H.-U. Demuth, *J. Neurochem.* **2012**, *121*, 774 – 784.
[9] W. He, C. J. Barrow, *Biochemistry* **1999**, *38*, 10871 – 10877.
[10] S. Schilling, T. Lauber, M. Schaupp, S. Manhart, E. Scheel, G. Böhm, H.-U. Demuth, *Biochemistry* **2006**, *45*, 12393 – 12399.
[11] J. O. Matos, G. Goldblatt, J. Jeon, B. Chen, S. A. Tatulian, *J. Phys. Chem. B* **2014**, *118*, 5637 – 5643.
[12] O. Wirths, C. Erck, H. Marten, A. Harmeier, C. Geumann, S. Jawhar, S. Kumar, G. Multhaup, J. Walter, M. Ingelsson et al., *J. Biol. Chem.* **2010**, *285*, 41517 – 41524.
[13] J. Nussbaum, J. Schilling, H. Cynis, A. Silva, E. Swanson, T. Wangsanut, K. Tayler, B. Wiltgen, A. Hatami, R. Rönicke, K. Reymann, B. Hutter-Paier, A. Alexandru, W. Jagla, S. Graubner, C. G. Glabe, H. U. Demuth, G. S. Bloom, *Nature* **2012**, *485*, 651 – 655.
[14] C. Russo, E. Violani, S. Salis, V. Venezia, V. Dolcini, G. Damonte, U. Benatti, C. D'Arrigo, E. Patrone, P. Carlo et al., *J. Neurochem.* **2002**, *82*, 1480 – 1489.
[15] P. Hortschansky, V. Schroeckh, T. Christopeit, G. Zandomeneghi, M. Fändrich, *Protein Sci.* **2005**, *14*, 1753 – 1759.
[16] N. Sun, R. Hartmann, J. Lecher, M. Stoldt, S. A. Funke, L. Gremer, H.-L. Ludwig, H.-U. Demuth, M. Kleinschmidt, D. Willbold, *J. Pept. Sci.* **2012**, *18*, 691 – 695.
[17] N. A. Whittemore, R. Mishra, I. Kheterpal, A. D. Williams, R. Wetzel, E. H. Serpersu, *Biochemistry* **2005**, *44*, 4434 – 4441.
[18] T. Lührs, C. Ritter, M. Adrian, D. Riek-Loher, B. Bohrmann, H. Döbeli, D. Schubert, R. Riek, *Proc. Natl. Acad. Sci. USA* **2005**, *102*, 17342 – 17347.
[19] Y.-H. Lee, Y. Goto, *Biochim. Biopys. Acta Proteins Proteomics* **2012**, *1824*, 1307 – 1323.
[20] T. P. J. Knowles, C. A. Waudby, G. L. Devlin, S. I. A. Cohen, A. Aguzzi, M. Vendruscolo, E. M. Terentjev, M. E. Welland, C. M. Dobson, *Science* **2009**, *326*, 1533 – 1537.
[21] W.-F. Xue, A. L. Hellewell, W. S. Gosal, S. W. Homans, E. W. Hewitt, S. E. Radford, *J. Biol. Chem.* **2009**, *284*, 34272 – 34282.
[22] C. Sachse, M. Fändrich, N. Grigorieff, *Proc. Natl. Acad. Sci. USA* **2008**, *105*, 7462 – 7466.
[23] C. Haupt, J. Leppert, R. Rönicke, J. Meinhardt, J. K. Yadav, R. Ramachandran, O. Ohlenschläger, K. G. Reymann, M. Görlach, M. Fändrich, *Angew. Chem. Int. Ed.* **2012**, *51*, 1576 – 1579; *Angew. Chem.* **2012**, *124*, 1608 – 1611.
[24] I. Bertini, L. Gonnelli, C. Luchinat, J. Mao, A. Nesi, *J. Am. Chem. Soc.* **2011**, *133*, 16013 – 16022.
[25] H. A. Scheidt, I. Morgado, S. Rothemund, D. Huster, M. Fändrich, *Angew. Chem. Int. Ed.* **2011**, *50*, 2837 – 2840; *Angew. Chem.* **2011**, *123*, 2889 – 2892.
[26] H. A. Scheidt, I. Morgado, S. Rothemund, D. Huster, *J. Biol. Chem.* **2012**, *287*, 2017 – 2021.
[27] I. Benilova, R. Gallardo, A. A. Ungureanu, C. V. Castillo, A. Snellinx, M. Ramakers, C. Bartic, F. Rousseau, J. Schymkowitz, B. De Strooper, *J. Biol. Chem.* **2014**, *289*, 30977 – 30989.

Received: November 30, 2015
Published online: March 11, 2016

  